ISSN 1054-660X, Laser Physics, 2007, Vol. 17, No. 8, pp. 1033–1036.

High Average Power and Short Pulse Duration Continuous Wave Mode-Locked Nd:GdVO$_4$ Laser with a Semiconductor Absorber Mirror

J. Y. Peng[a, c, *], B. S. Wang[a, c], Y. G. Wang[b], J. G. Miao[a, c], E. J. Hao[a, c], H. M. Tan[a], L. S. Qian[a], and X. Y. Ma[b]

[a] *Changchun Institute of Optics, Fine Mechanics, and Physics, Chinese Academy of Science, Changchun, 130022 China*

[b] *Institute of Semiconductors, Chinese Academy of Science, Beijing, 100083 China*

[c] *Graduate School of the Chinese Academy of Science, Beijing, 100039 China*

e-mail: jiyingpeng111@163.com

Received November 17, 2006

Abstract—Passive mode locking of a solid-state Nd:GdVO$_4$ laser is demonstrated. The laser is mode locked by use of a semiconductor absorber mirror (SAM). A low Nd^{3+} doped Nd:GdVO$_4$ crystal is used to mitigate the thermal lens effect of the laser crystal at a high pump power. The maximum average output power is up to 6.5 W, and the pulse duration is as short as 6.2 ps. The optic-to-optic conversion efficiency is 32.5% and the repetition rate is about 110 MHz.

PACS numbers: 42.55.Rz, 42.55.Xi, 42.60.Fc

DOI: 10.1134/S1054660X07080026

1. INTRODUCTION

In recent years, there has been significant interest in the use of semiconductor saturable absorbers to produce ultrafast optical pulses from solid-state lasers [1–5]. One of the important frontiers is the high average power [6]. Picosecond high-power diode-pumped solid-state lasers with good beam quality are attracting growing interest because of numerous applications in medicine, material processing, and nonlinear frequency conversion. For high-power lasers, the new laser crystal Nd:GdVO$_4$ is a better choice, because of its good physical, optical, and mechanical properties [7, 8]. Its broad absorption band and large absorption coefficient make it suitable for diode pumping. Its broad emission bandwidth is necessary for generating a narrow mode-locking pulse duration. Its short upper-state lifetime is efficient in suppressing the Q-switching instabilities. Most importantly, the Nd:GdVO$_4$ crystal has an unexpectedly high thermal conductivity, comparable to that of Nd:YAG and much higher than that of Nd:YVO$_4$, which provides the desirable advantage for high-power lasers. Several mode-locked Nd:GdVO$_4$ lasers have been demonstrated with semiconductor saturable absorber mirrors [8–10]. With single LD pumping, one group has achieved an average output power of 5.4 W with a pulse duration of 9.2 ps [9], and another group has achieved an average output power of 4.9 W with a pulse duration of 11.5 ps [10]. The thermal lens effect of the laser crystal and the SESAM damage were the main reasons for limiting the average output power. In this experiment, we used a super SAM as the saturable absorber, which had a high damage threshold; moreover, we used a low Nd^{3+} doped Nd:GdVO$_4$ crystal and designed the laser cavity elaborately to mitigate the effect of the thermal lens. Finally, we achieved a high average output power of 6.5 W at the maximum incident pump power in the cw mode-locking operation; the optic-to-optic conversion efficiency was about 32.5%. The pulse duration was as short as 6.2 ps and the repetition rate was about 110 MHz.

2. EXPERIMENTAL SETUP

The SAM was grown on a GaAs substrate by metal-organic chemical-vapor deposition. The SAM consisted of 22 pairs of GaAs/AlAs quarter-wave Bragg layers with a high reflectivity of 99.5% at the lasing wavelength of 1063 nm and a 15-nm relaxed In$_{0.3}$Ga$_{0.7}$As single quantum well (embedded in the topmost layer of the Bragg stack) to achieve saturable absorption at 1063 nm. The Bragg layers and the In$_{0.3}$Ga$_{0.7}$As absorber were grown at temperatures of 720 and 500°C, respectively. To achieve a high damage threshold, the SAM was coated with three pairs of SiO$_2$/Al$_2$O$_3$ as the protective film and the reflectivity was about 50%. The In$_{0.3}$Ga$_{0.7}$As absorber was grown at low temperature 500°C for a fast recovery time. The structure is shown in detail in Fig. 3.

The cavity configuration is shown in Fig. 1. The Nd^{3+} concentration of the laser crystal was 0.5 at. %, and its length was 5.5 mm. The laser crystal was wrapped with indium foil and mounted in a copper

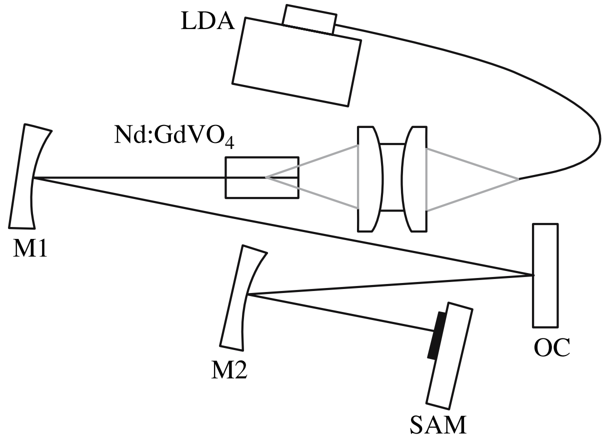

Fig. 1. Configuration of the mode-locked Nd:$GdVO_4$ laser with a SAM.

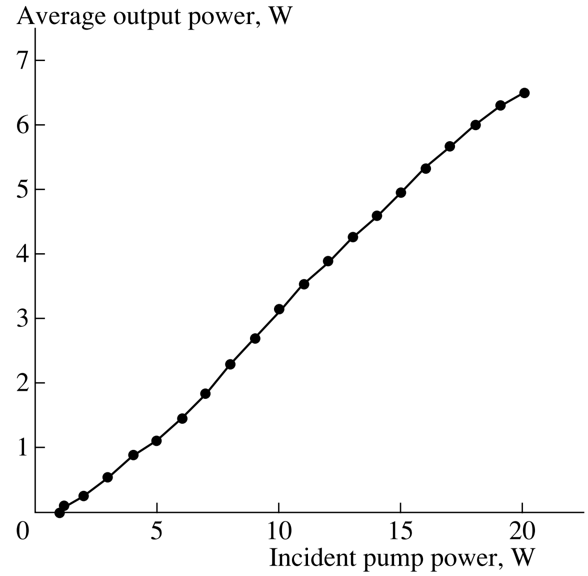

Fig. 2. The average output power as a function of the incident pump power.

block cooled by a thermoelectric cooler. One side of the laser crystal was antireflection coated for a 808-nm (T > 98%) pump wavelength and high reflection (R > 99.8%) for the 1063-nm lasing radiation, while the other side was antireflection coated for 1063 nm. The pump source was a 20-W fiber-coupled laser diode with a core diameter of 0.4 mm and a numerical aperture of 0.22. The central wavelength of the LD was 810.2 nm at 25°C and can be tuned by changing the working temperature of the LD to match the best absorption of the laser crystal. The fiber output was focused onto the laser crystal and the pump spot radii was about 200 μm. The resonator consisted of two highly reflective (at 1063 nm) mirrors, M1 and M2; one partially reflective (PR) mirror; an output coupler (OC); a laser crystal; and a SAM. The OC is a flat mirror; the radii of curvature for M1 and M2 are 500 and 200 mm, respectively. The OC had a reflectivity of 90% at 1063 nm, giving a total output coupling of 19%. The total cavity length was about 1350 mm. M1 and M2 were separated by about 920 mm. The mode radii in the crystal were about 140–160 μm. The mode radii on the SAM was approximately 40–60 μm. The SAM was simply mounted on a copper heat sink, but no active cooling was applied.

3. RESULTS AND DISCUSSION

The behavior of the laser's average output power as a function of the incident pump power was investigated as shown in Fig. 2. The oscillation threshold was about 1.2 W. The low threshold indicated that the SAM did not induce significant nonsaturable losses. Near the oscillation threshold, the output was effectively cw; slightly increasing the pump power initiated a Q-switched mode-locked (QML) state. The temporal behavior of the laser pulses was recorded by a fast response InGaAs photodiode with a time resolution of 0.5 ns and a LeCroy oscilloscope (9361C). The QML pulse train is shown in Fig. 3. The repetition rate of the Q-switched envelope increased from 200 to 300 kHz as the incident pump power increased from 2.5 to 10 W. The pulse width of the Q-switched envelope was about 1 μs. When the pump power increased to about 10 W, the QML state is transformed into a cw mode-locked (CML) state. At a pump power of 10 W, the average output power was about 3.14 W. Figures 4 and 5 show the CW mode-locked pulse trains in different time divisions, respectively. The repetition rate was about 110 MHz. At the maximum incident pump power of 20 W, an average output power of 6.5 W was obtained. The optical–optical conversion efficiency was about 32.5%. Also at a pump power of 20 W, the pulse width of the CW mode-locked laser output was measured by a

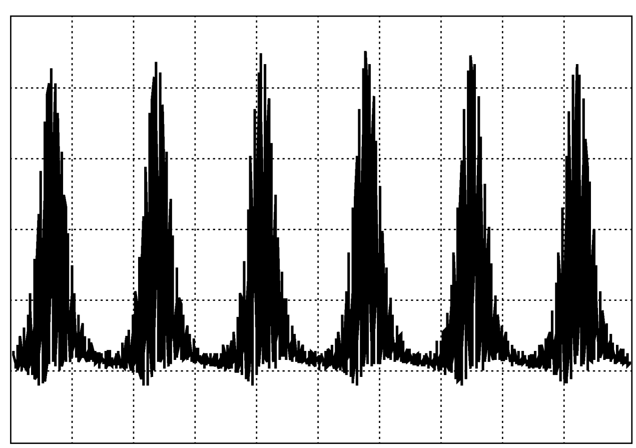

Fig. 3. Q-switched mode-locked pulse train (2 μs/div).

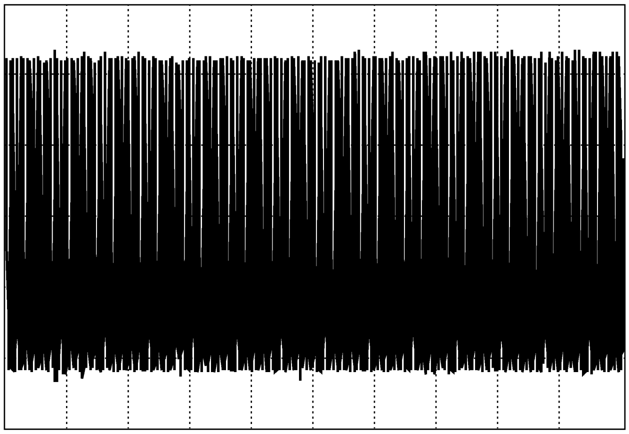

Fig. 4. CW mode-locked pulse train (2 μs/div).

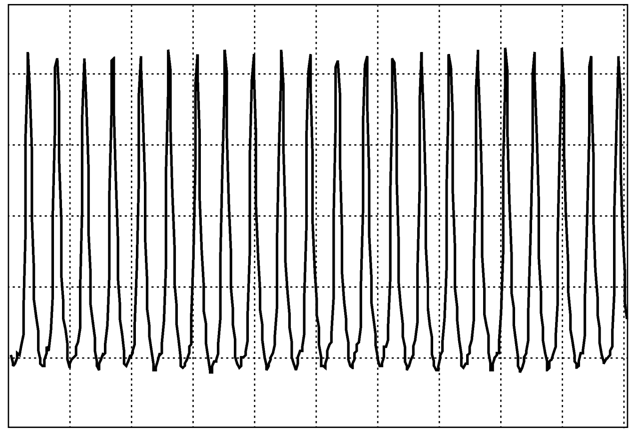

Fig. 5. CW mode-locked pulse train (20 ns/div).

homemade autocorrelator with a 3-mm-long KTP crystal under a type-II phase-matched second-harmonic interaction in a collinear configuration. The autocorrelation trace is shown in Fig. 6. The pulse width was about 6.2 ps assuming a Gaussian pulse shape. The optical spectrum was measured by a Spectrum Analyzer (AQ 6317B). The spectrum was centered at 1062.8 nm with a FWHM bandwidth of about 0.49 nm with a slight asymmetric spectral distribution. In our opinion, the etalon effect from the two end surfaces of the laser crystal led to the asymmetric spectral profile. The time–bandwidth product was calculated to be 0.8, indicating a chirped pulse. Probably, the SAM recovery time or the crystal dispersion that limited the mode-locked pulse. To measure the laser beam quality factor M^2, the beam was focused with a planoconcave lens (f = 200 mm). The laser beam quality factor M^2 was measured to be about 1.33 for the sagittal plane and 1.38 for the tangential plane using the knife-edge technique [11]. No damage to the SAM was observed over several hours of operation, which indicated a high damage threshold of the super SAM. The average output power always increased along with an increased incident pump power and the optical–optical conversion efficiency (32.5%) was relatively high, which indicated a logical cavity design.

It is worthwhile analyzing the thermal lens in the Nd:$GdVO_4$ crystal, which affects the output power of the laser and the stability of the resonator. For a laser pumped by a fiber-coupled diode, the focal length of the thermal lens f_{th} can be approximately given by [12, 13]. The focal length of the thermal lens was found to be about 65 mm at a pump power of 20 W. Considering the thermal lens effect, we designed a thermal-stable cavity. The cavity was designed to easily allow mode matching with the pump beam and to provide the proper spot size on the SAM. The mode radii in the laser crystal were about 140–160 μm (0.7–0.8 times the pump size). The mode radii on the SAM were approximately 40–60 μm. The mode radii were calculated using the laser transfers matrix. As far as we know, when the incident power was increased, the thermal lens effect became more serious. In this case, to keep the mode matching precise and to achieve a high conversion efficiency, the distance between mirror M2 and the SAM should be changed slightly. The distance was determined to be 100–103 mm.

The Nd^{3+} doped concentration of the Nd:$GdVO_4$ crystal influences the thermal lens effect of the gain medium. In [9], a 1.3% Nd^{3+} doped Nd:$GdVO_4$ crystal was used and, in [10], the Nd^{3+} doped concentration was 1.0%. In order to weaken the thermal effect, we selected a 0.5% Nd^{3+} doped Nd:$GdVO_4$ as the gain medium. The lengths of the crystal were 3 and 4 mm, respectively, in the above two experiments. To increase

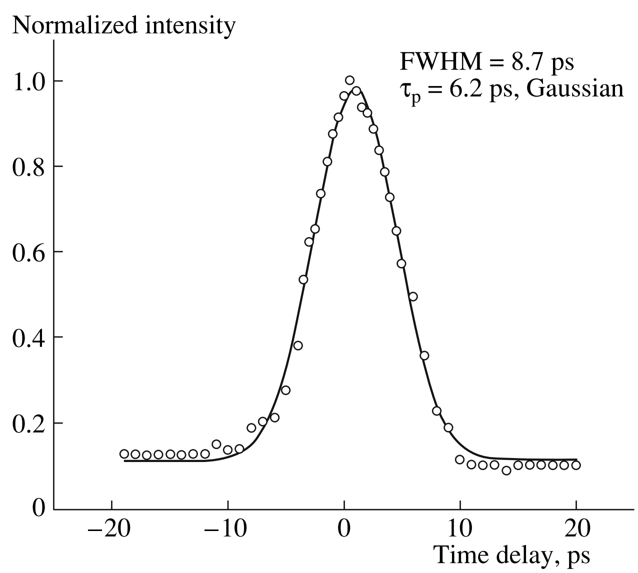

Fig. 6. Autocorrelation trace of the output pulses from the CW mode-locked Nd:$GdVO_4$ laser.

the gain of the laser crystal, we chose a longer (5.5 mm) crystal in this experiment. The average output power was higher than that of the above two experiments. As for the SAM, to achieve a high damage threshold, it was coated with three pairs of SiO_2/Al_2O_3 as the protective film, and, to get a high modulation depth, the $In_{0.3}Ga_{0.7}As$ absorber layer was thickened to be 15 nm. In [8], the SAM absorber layer was 12 nm, and an 8-ps mode-locking pulse duration was obtained. In this experiment, with the super SAM, we achieved a shorter pulse duration of about 6.2 ps and the SAM was not damaged at a high power output.

5. CONCLUSIONS

A high-power diode-end-pumped cw mode-locked $Nd:GdVO_4$ laser was demonstrated with a super SAM as the mode-locking absorber. The low insertion loss, high modulation depth, and high damage threshold indicated that the SAM was suitable for high power and narrow pulse width mode-locked lasers. Considering the thermal lens effect, we chose a low Nd^{3+} doped $Nd:GdVO_4$ crystal and elaborately designed the laser cavity. Finally, a high average power of 6.5 W and a short pulse duration of 6.2 ps were obtained at a pump power of 20 W. The pulse repetition rate was about 110 MHz. The Q-switching instability was well suppressed and the cw mode-locked pulse train was stable.

REFERENCES

1. U. Keller, D. A. B. Miller, G. D. Boyd, et al., Opt. Lett. **17**, 505 (1992).
2. R. Paschotta, J. Aus der Au, G. J. Spuhler, et al., Appl. Phys. B **70**, S25 (2000).
3. A. Major, N. Langford, T. Graf, et al., Opt. Lett. **27**, 1478 (2002).
4. J. L. He, Y. X. Fan, J. Du, et al., Opt. Lett. **29**, 2803 (2004).
5. J. Du, X. Y. Liang, Y. G. Wang, et al., Opt. Express **13**, 7970 (2005).
6. U. Keller, Nature **424**, 831 (2003).
7. P. A. Studennikin, A. I. Zagumennyi, Y. D. Zavartsev, et al., Quantum Electron. **25**, 1162 (1995).
8. B. Y. Zhang, G. M. Chen, et al., Opt. Lett. **28**, 1829 (2003).
9. J. L. He, C.-K. Lee, J.Y. Huang, et al., Appl. Opt. **42**, 5496 (2003).
10. S. J. Zhang, E. Wu, H. F. Pan, and H. P. Zeng, IEEE J. Quantum Electron. **40**, 505 (2004).
11. A. E. Siegman, M. W. Sasnett, T. F. Johnston, IEEE J. Quantum Electron. **27**, 1098 (1991).
12. M. E. Innocenzi, H. T. Yura, C. Fincher, and R. A. Fieids, Appl. Phys. Lett. **56**, 1831 (1990).
13. F. Song, C. B. Zhang, X. Ding, et al., Appl. Phys. Lett. **81**, 2145 (2002).